ELSEVIER

Applied Catalysis A: General 260 (2004) 55–61

A: GENERAL

www.elsevier.com/locate/apcata

XPS study of multiwall carbon nanotube synthesis on Ni-, V-, and Ni, V-ZSM-5 catalysts

Zoltán Kónya [a], István Vesselényi [a], János Kiss [b], Arnold Farkas [b], Albert Oszkó [b], Imre Kiricsi [a,*]

[a] *Department of Applied and Environmental Chemistry, University of Szeged, H-6720 Szeged, Rerrich Béla tér 1, Hungary*
[b] *Reaction Kinetics Research Group of the Hungarian Academy of Sciences, University of Szeged, H-6701 Szeged, P.O. Box 168, Hungary*

Received in revised form 5 October 2003; accepted 7 October 2003

Abstract

The present text describes an investigation of XPS study of multiwall carbon nanotube (MWNT) synthesis. The aim of the investigation was not only to improve the reaction activity by mixing nickel with vanadium, but also to understand the formation mechanism of the nanotubes. Carbon nanotubes were produced by catalytic chemical vapor deposition (CCVD) of acetylene on transition metal containing catalysts supported on zeolite ZSM-5. The samples were characterized at two different levels. At the nanoscale, they were studied by transmission electron microscopy (TEM), while at macroscopic scale mainly XPS was used to investigate the changes during the reaction.

Keywords: Multiwall carbon nanotubes; Chemical vapor deposition; Transition metal containing catalysts

1. Introduction

The discovery of multiwall carbon nanotubes (MWNTs) by Iijima [1]; and the singlewall carbon nanotubes (SWNTs) by Iijima and Ichihashi [2] and Bethune et al. [3] more than a decade ago marked the opening of a new chapter in nano-scale materials science. Active research followed that discovery, mainly on the formation and properties of these quasi one-dimensional tubular structures. Several production methods have been developed aiming at the production of carbon nanotubes in large scale, such as laser vaporization [4], electric arc discharge [5] and catalytic chemical deposition of hydrocarbons over metal catalysts (CCVD technique) [6], however, only the latter method supplies carbon nanotubes in high yield at a low cost of production. In the catalytic process, the combinations of transition metals and supports can be changed depending on the characteristics required, for example the alignment [7] or the size of the tubes [8,9].

Although the formation mechanism of MWNTs on heterogeneous catalysts is well documented, some fundamental questions are still unsolved, such as: (i) the nature of interactions between the support and the metals, (ii) the electronic state of the metals, and (iii) the interaction of the different metals in the bimetallic catalysts. Recently, we proved by XPS [10] and Mössbauer spectroscopy [11] that in case of iron and cobalt containing bimetallic catalysts CoFe alloy formation occurred during the reaction towards MWNT synthesis.

In this presentation, we focus on the characterization of the chemical state of nickel and vanadium containing mono- and bi-metallic catalysts before and after acetylene treatments by in situ XPS method. Samples were analyzed by XPS, infrared spectroscopy (IR), and X-ray diffraction (XRD). The formed carbonaceous products were characterized by transmission electron microscopy (TEM) and TG techniques, as well.

2. Experimental

2.1. Preparation of the catalyst

All catalysts were prepared by impregnation of the support with ethanolic solution of the respective metal salt (metal salt used were nickel acetate and vanadium acetyl acetonate) or their binary mixture. The concentration of metal was 5 wt.%

* Corresponding author. Tel.: +36-62544478; fax: +36-62544619.
E-mail address: kiricsi@chem.u-szeged.hu (I. Kiricsi).

0926-860X/$ – see front matter © 2003 Elsevier B.V. All rights reserved.
doi:10.1016/j.apcata.2003.10.042

in single metal containing catalyst and 2.5–2.5 wt.% in the binary metal mixture catalyst.

2.2. Synthesis and in situ characterization of the catalysts by XPS

The XPS experiments were performed in an ultra-high vacuum system with a background pressure of 10^{-9} mbar, produced by an ion getter pump. The photoelectrons generated by Al K_α primary radiation (15 kV, 15 mA) were analyzed with a hemispherical electron energy analyzer (Kratos XSAM 800). The pass energy was set to 40 eV. An energy step width of 50 meV and a dwell time of 300 ms were used. Typically 10 scans were accumulated for each spectrum. Fitting and deconvolution of the spectra were performed with the help of VISION software. All binding energies were referenced to Al(2p) at 74.7 eV. For analyses the O(1s), C(1s), Ni(2p), and V(2p) core electrons were chosen.

Briefly, zeolites ZSM-5 impregnated with Ni^{2+}, V^{4+}, and Ni^{2+}/V^{4+} salts were analyzed by XPS after the following treatments. The samples were first evacuated at 300 K in the XPS chamber (treatment A). After evacuation heat treatment at 973 K was carried out in the sample handling chamber, excluding the contamination with air or moisture preceding the XPS measurement (treatment B). The samples were then cooled to 300 K and acetylene was introduced into the chamber. Equilibrating the samples in acetylene atmosphere was performed for 20 min followed by evacuation (treatment C). Finally the samples were reacted in acetylene at 973 K for 20 min (treatment D). Each treatment was carried out in a special sample handling chamber assuring the transfer of the samples into the analysis chamber under exclusion of air or moisture contamination.

2.3. Characterization of the obtained carbon materials

The production of nanotubes was carried out at 973 K during 1 h using acetylene flow of 30 ml/min and N_2 flow of 300 ml/min as carrier gas. After reaction the system was cooled down to room temperature and the product was analyzed by TEM. For TEM and HRTEM Philips CM20 and JEOL 200CX were used. For the preparation of sample holder grids, the glue technique was used described elsewhere in details [12]. Adsorption and desorption of nitrogen was measured at 77 K in a volumetric system in the whole relative pressure range. From the isotherms the BET surface area and the pore size distribution of samples were determined. Pore size distributions were calculated by the Barrett–Joyner–Halenda method [13] in order to get more insight into the mesoporous structures.

3. Results and discussion

3.1. Adsorption results

BET surface data for all the samples are presented in Table 1. A significant decrease in the specific surface area values is observable after nanotube formation.

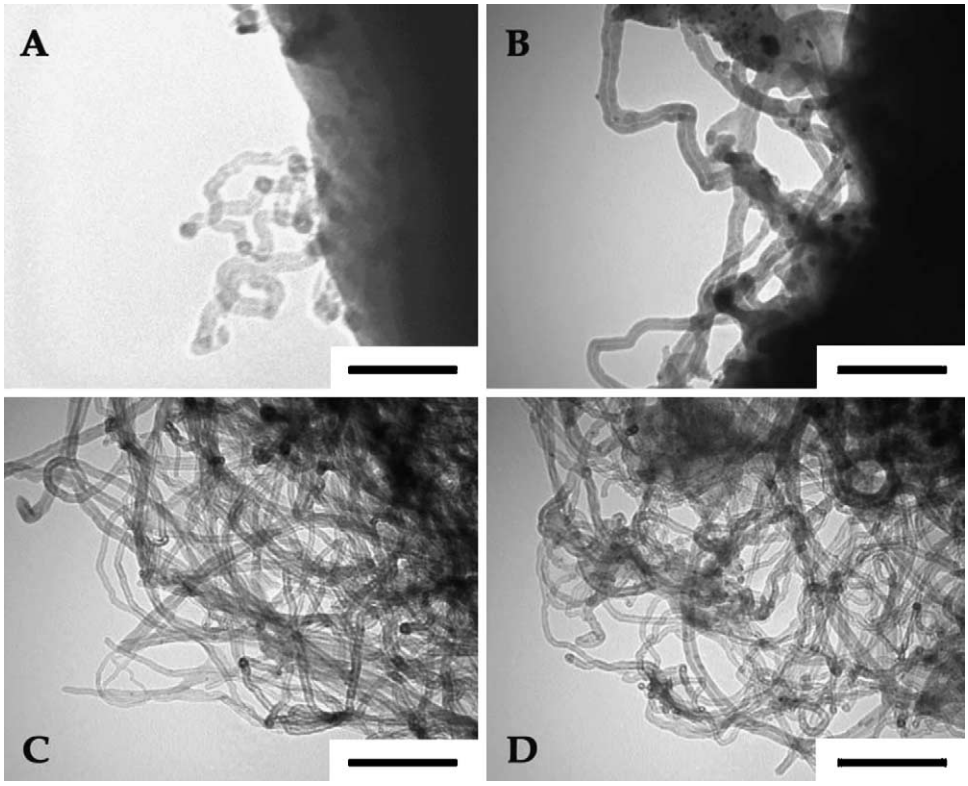

Fig. 1. TEM images of catalyst treated at 1000 K for 60 min in acetylene: Ni-ZSM-5 (a), V-ZSM-5 (b), and Ni,V-ZSM-5 (c).

Table 1
Nitrogen porosimetry results

Sample	BET area (m^2/g)
Na-ZSM-5[a]	287.1
Ni-ZSM-5a	241.3
Ni-ZSM-5 + MWNTs[b]	199.6
V-ZSM-5a	274.9
V-ZSM-5 + MWNTs[b]	157.5
Ni,V-ZSM-5[a]	266.6
Ni,V-ZSM-5 + MWNTs[b]	167.1

[a] The sample is calcined in nitrogen atmosphere.
[b] After nanotube formation.

3.2. TEM results

TEM images were taken on the catalyst samples treated in in situ XPS experiments in order to reveal the differences of carbon nanostructures generated. Fig. 1 shows three TEM pictures taken on the Ni-ZSM-5, V-ZSM-5, and Ni,V-ZSM-5 samples after in situ reaction with acetylene at 1000 K for 60 min. On Ni containing monometallic sample carbon nanotubes were produced (Fig. 1a), while no nanotube formation was observed on supported vanadium catalyst where the structure on the image is more characteristic of carbon fibres (Fig. 1b). Oppositely, the carbon product formed on Ni,V-ZSM-5 bi-metallic catalyst is completely different from those obtained on mono-metallic samples. Here well structured carbon nanotubes can be seen (Fig. 1c).

As it will be shown later, the TEM observation is in good agreement with the XPS results where high quality carbon nanotube formation will be proven on the bi-metallic catalyst, and the role of the presence of vanadium will be explained.

3.3. XPS spectroscopy

3.3.1. Ni-ZSM-5 sample

Spectrum of sample treated by method A showed a typical oxide structure (Fig. 2a). The split 2p electron energy levels Ni($2p_{3/2}$) and Ni($2p_{1/2}$) appeared at 855.8 and 873.6 eV, respectively. These bond energies are higher here by 1.5–2.0 eV compared to the pure NiO [14]. This deviation was probably due to the difference in coordination of Ni^{2+} in zeolite and in NiO. It is very probable that Ni^{2+} ions are coordinated in much higher symmetry

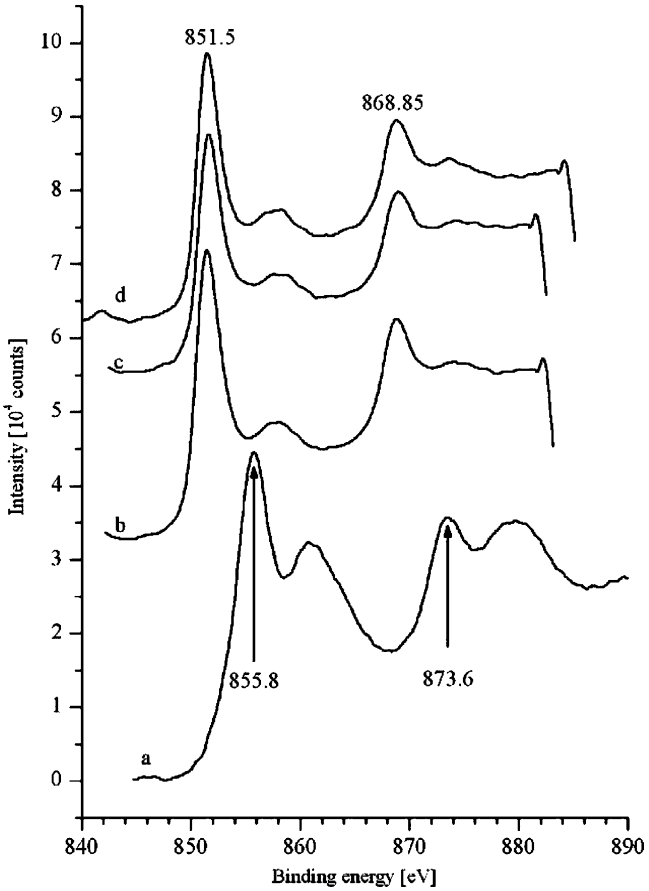

Fig. 2. XP spectra of Ni-ZSM-5 in Ni(2p) region (a) after evacuation at 300 K for 60 min, (b) after calcination at 1000 K for 20 min, (c) after 2.666 kPa C_2H_4 adsorption at 300 K for 60 min, and (d) after interaction with 2.666 kPa C_2H_4 at 1000 K for 60 min.

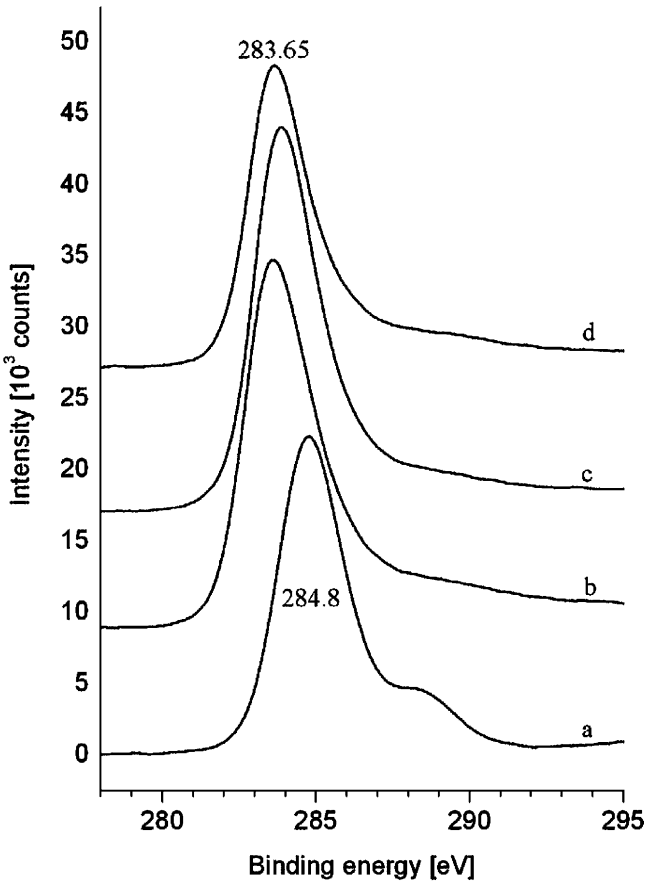

Fig. 3. XP spectra of Ni-ZSM-5 in C(1s) region (a) after evacuation at 300 K for 60 min, (b) after calcination at 1000 K for 20 min, (c) after 2.666 kPa C_2H_4 adsorption at 300 K for 60 min, and (d) after interaction with 2.666 kPa C_2H_4 at 1000 K for 60 min.

in zeolites possessing well ordered crystal structure than in NiO. The typical oxide structure is also supported by the satellite appearing at higher bond energy values. Significant change occurred in the state of nickel upon heat treatment at 973 K (Fig. 2b). Ni($2p_{3/2}$) appeared at 851.5 eV characteristic of metallic nickel, the satellite bonds due to NiO disappeared, the whole spectrum shows a metallic structure [14,15] and this character does not change even upon treatment C as can be seen in Fig. 2c. For Ni-ZSM-5 sample the XPS spectral changes suggest that, Ni^{2+} ions are reduced upon heat treatment in vacuum at 973 K, and Ni remains in this metallic state after treatment in acetylene at 973 K (Fig. 2d).

The C(1s) spectrum taken after treatment A shows a bond at 284.75 eV, pointing to some carbon impurities left behind after catalyst preparation. After treatment B (Fig. 3b) the position of C(1s) band shifted by 1 eV to the lower energies, indicating the formation of polymeric or graphitic carbon. This peak was not changed even after heat treatment at 973 K.

In the O(1s) spectra (Fig. 4) a symmetric band was found at 532.2 eV. The positions of oxygen binding energies did not change after any treatment, reflecting that they are determined mainly by the zeolitic oxygen being structure constituents of the zeolite crystal.

3.3.2. V-ZSM-5 sample

The changes in the state of vanadium was followed by the $2p_{3/2}$ (and $2p_{1/2}$) transitions, however, for the latter the O(1s) satellite signal partially overlapping). After treatment A vanadium is in oxidized state, the $2p_{3/2}$ signal appears at 516.5 eV (see Fig. 5a). As this peak is rather broad, the combination of two photoemission transitions cannot be excluded. Demeter reported that in V_2O_5 the V($2p_{3/2}$) appeared at 517.2 eV, while in VO_2 a similar energy level could be observed (518.85 eV) [16]. Analogous conclusions were reported by Choi [17]. Considering these we assume that the vanadium has two different, namely V^{4+} and V^{5+} oxidation states. The C(1s) spectrum of this stage reveals that some carbon remained in the sample after preparation (Fig. 6a). The O(1s) energy level appeared at 538.3 eV characteristic of the zeolitic oxygen (Fig. 7a).

Substantial changes can be observed in the V(2p), C(1s), and O(1s) spectra taken after treatment B. The most

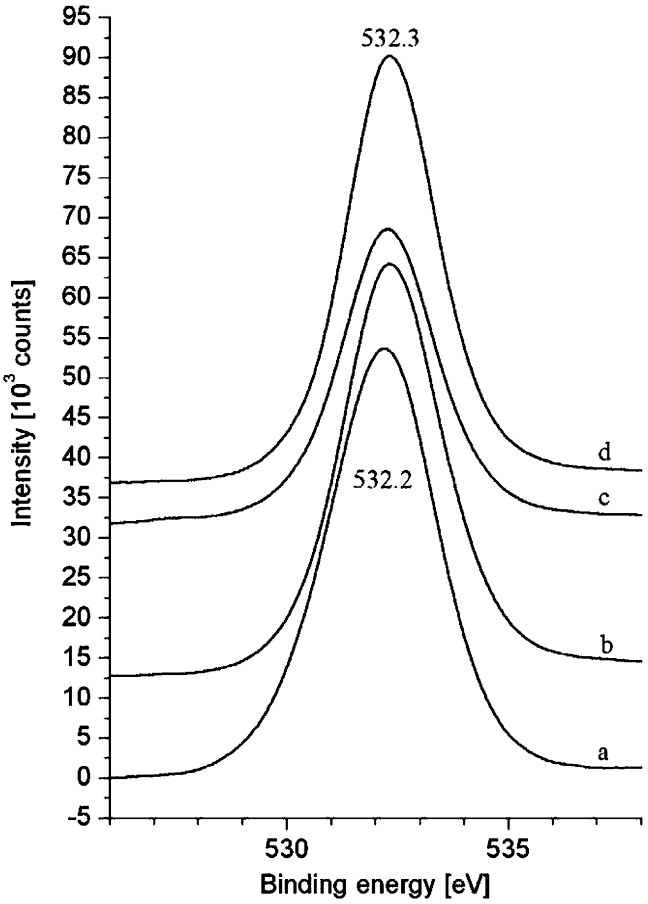

Fig. 4. XP spectra of Ni-ZSM-5 in O(1s) region (a) after evacuation at 300 K for 60 min, (b) after calcination at 1000 K for 20 min, (c) after 2.666 kPa C_2H_4 adsorption at 300 K for 60 min, and (d) after interaction with 2.666 kPa C_2H_4 at 1000 K for 60 min.

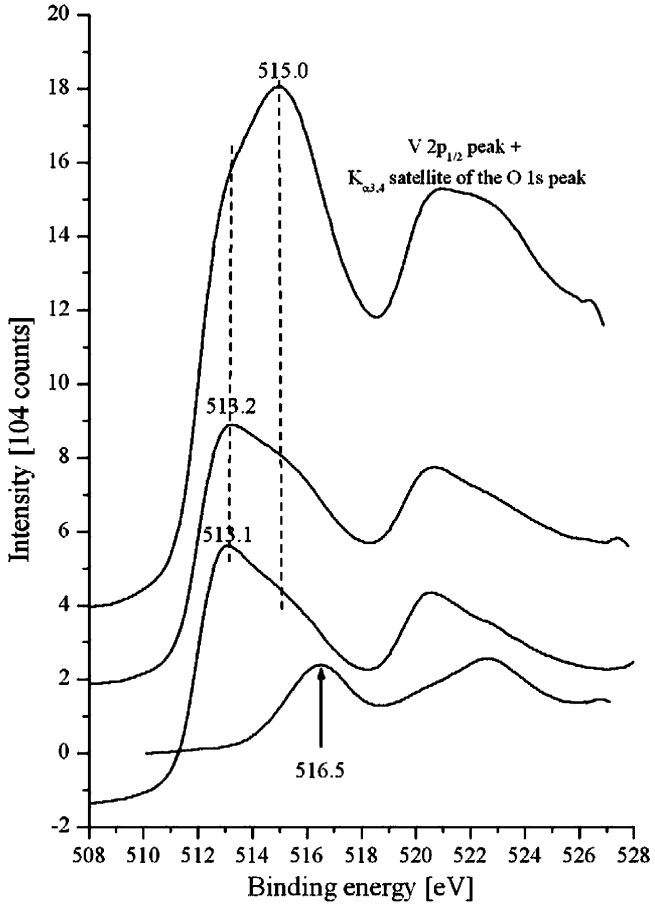

Fig. 5. XP spectra of V-ZSM-5 in Ni(2p) region (a) after evacuation at 300 K for 60 min, (b) after calcination at 1000 K for 20 min, (c) after 2.666 kPa C_2H_4 adsorption at 300 K for 60 min, and (d) after interaction with 2.666 kPa C_2H_4 at 1000 K for 60 min.

significant change is seen in the V(2p) spectrum. The transition due to the higher oxidation state decreases and shifted to lower binding energies and the signal became asymmetric. The transitions appear at 513.1 eV (more intensive) and 515.0 eV. Similar spectrum was obtained after treatment C, however, in this case, the asymmetry of the transitions changed; the signal at 515.0 eV became more intensive.

To the interpretation of these changes we should discuss the changes in C(1s) spectrum (Fig. 6). Upon calcination and acetylene exposure a new transition at 282.3 eV appeared. This is an indication for the carbide formation [17]. Considering this we attribute the V($2p_{3/2}$) peak at 513.2 eV to vanadium carbide (VC). Choi [17]has investigated the structure of VC using XPS, and evidenced that V($2p_{3/2}$) transition can be found at 513.2 eV in VC17.

In our C(1s) spectra a high intensity signal emerged at 284.4 eV and was assigned as graphitic carbon following Choi's [17]work. The binding energy at 515.0 eV due to V($2p_{3/2}$) can be attributed to a mixture of vanadium oxides (V_xO_y) generated upon heat and acetylene treatments. As we have mentioned Demeter et al. found the transition of V^{3+} V($2p_{3/2}$) at 515.8 eV [16]. From this it follows that the reduction of vanadium ions is not complete. A part of them is reduced to VC (513.2 eV). A significant part of vanadium may incorporate into the ZSM-5 zeolitic structure [18,19]. There are several literature data proving the movement of vanadium from extraframework to framework position upon heat treatment at high temperatures [20,21]. The change of the oxidation state of vanadium species has also been reported [22].

As the O(1s) spectra show (Fig. 7), beside the binding energy at 532.3 eV characteristic of zeolitic oxygen, a new transition appeared at 530.15 eV. This signal is attributed to the oxygen in mixed V_xO_y oxides. As this oxygen signal has relatively high intensity, it suggests that vanadium ions stabilized in the zeolite should situate in the outer surface detectable by XPS.

Considering the experimental results obtained for V-ZSM-5 sample the following summary can be given. In contrast to the nickel containing sample vanadium cannot be reduced completely, and formation of VC was proven. As an overlay on VC, the presence of graphitic carbon was also evidenced. Vanadium is presented in two different

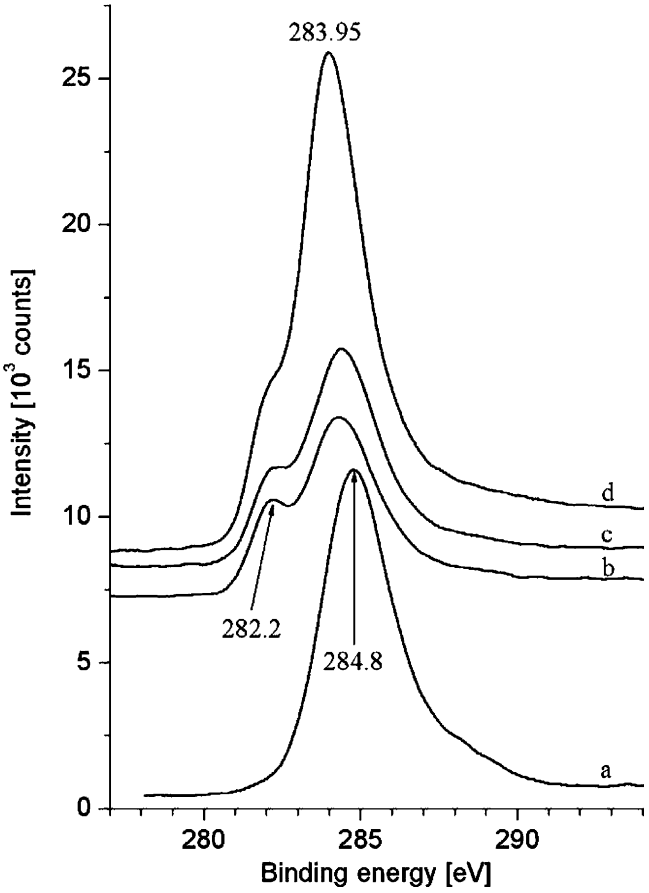

Fig. 6. XP spectra of V-ZSM-5 in C(1s) region (a) after evacuation at 300 K for 60 min, (b) after calcination at 1000 K for 20 min, (c) after 2.666 kPa C_2H_4 adsorption at 300 K for 60 min, and (d) after interaction with 2.666 kPa C_2H_4 at 1000 K for 60 min.

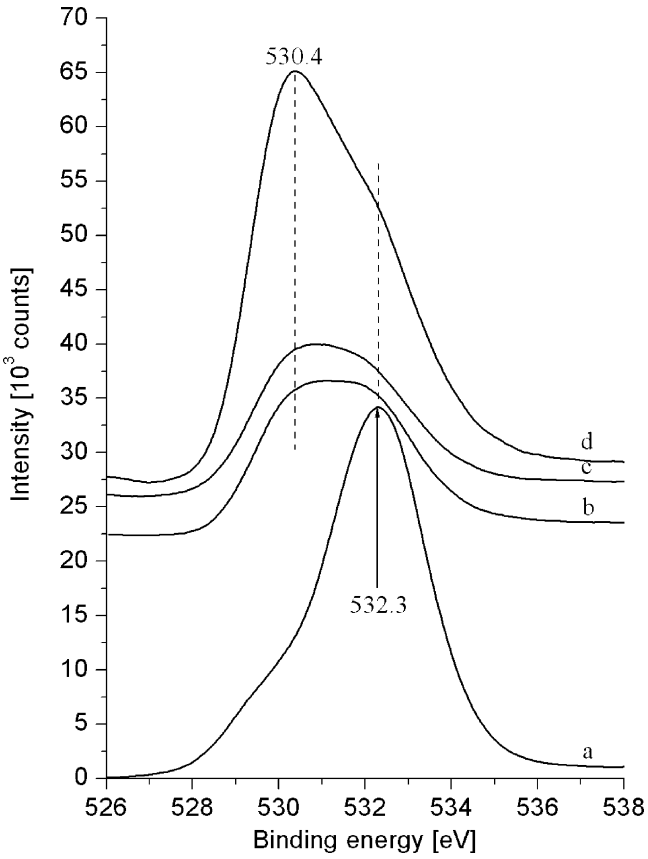

Fig. 7. XP spectra of V-ZSM-5 in O(1s) region (a) after evacuation at 300 K for 60 min, (b) after calcination at 1000 K for 20 min, (c) after 2.666 kPa C_2H_4 adsorption at 300 K for 60 min, and (d) after interaction with 2.666 kPa C_2H_4 at 1000 K for 60 min.

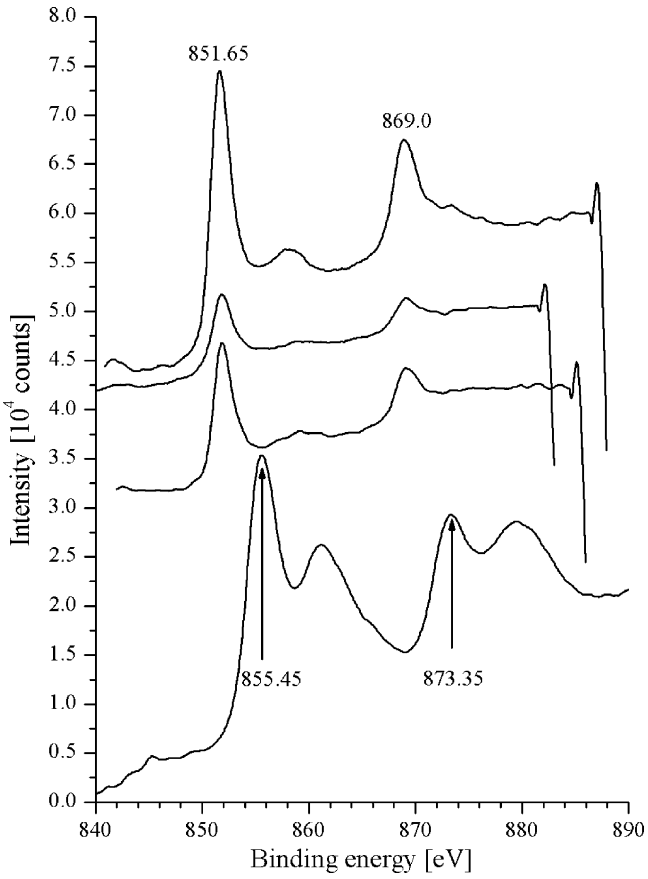

Fig. 8. XP spectra of Ni,V-ZSM-5 in Ni(2p) region (a) after evacuation at 300 K for 60 min, (b) after calcination at 1000 K for 20 min, (c) after 2.666 kPa C_2H_4 adsorption at 300 K for 60 min, and (d) after interaction with 2.666 kPa C_2H_4 at 1000 K for 60 min.

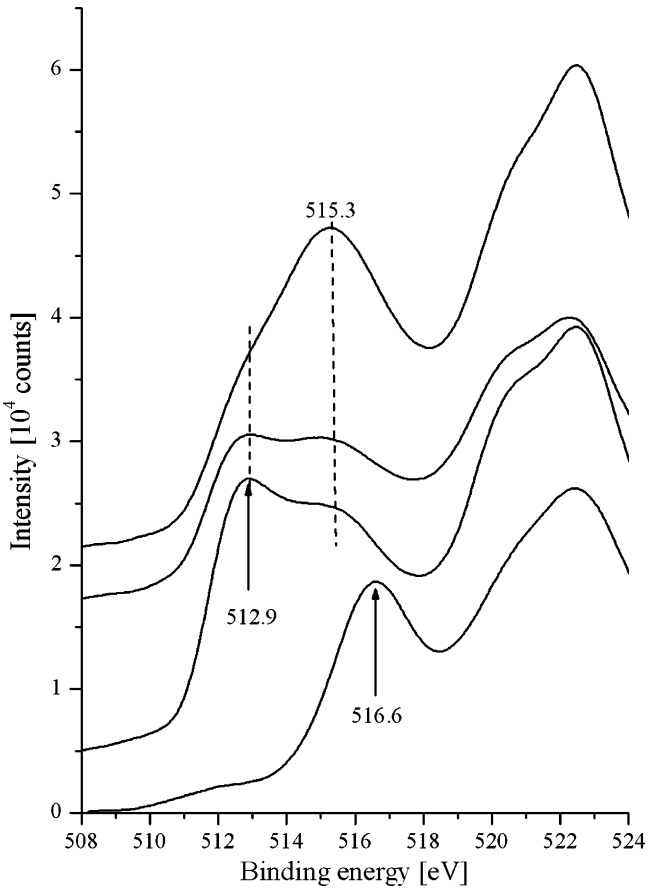

Fig. 9. XP spectra of Ni,V-ZSM-5 in V(2p) region (a) after evacuation at 300 K for 60 min, (b) after calcination at 1000 K for 20 min, (c) after 2.666 kPa C_2H_4 adsorption at 300 K for 60 min, and (d) after interaction with 2.666 kPa C_2H_4 at 1000 K for 60 min.

oxidation states and a part of the vanadium is incorporated into the zeolitic framework.

3.3.3. *Ni,V-ZSM-5 sample*

It is worth mentioning here again that the highest conversion of acetylene was achieved on this catalyst and well graphitized carbon nanotubes were formed. As it is seen in Fig. 8, the state of nickel changes identical way as has been obtained for Ni-ZSM-5 sample.

The energy levels of V(2p) due to the presence of V^{4+} and V^{5+} oxidation state are shifted to the lower binding energies, however, the extent of shifts slightly changed in presence of nickel. For Ni,V-ZSM-5 the positions of V(2p) are at 515.3 and 521.8 eV (Fig. 9). In the absence of nickel these energy levels appeared at 525.0 and 513.2 eV, respectively. These data suggest that more vanadium with higher oxidation states may chemically bond to the zeolite structure. The most significant difference between spectra taken in the absence and in the presence of Ni is that no transition characteristic of VC binding energy at 513.2 eV was observed in the latter case. Instead, a lower energy transition emerged at 512.8 eV, which binding energy is characteristic of the metallic vanadium [16,17]. From this it follows that metallic vanadium is formed in the presence of nickel and no VC is generated.

The former assumption is supported by the C(1s) spectra as well (Fig. 10). For Ni,V-ZSM-5 sample the binding energy of C(1s) at 282.4 eV due to VC was not observed. Consequently, no VC formation can be considered in this sample.

The O(1s) XPS signals are depicted in Fig. 11. In the absence of nickel two separated binding energies were detected at 532.2 and 530 eV. However, the transition of lower energy was not detected in the presence of nickel. This suggests that the presence of nickel changes the distribution of VO groups at the surface layer.

Summarizing the XPS results for Ni,V-ZSM-5 catalyst, we can state that the changes of the state of nickel followed the same tendency as for Ni-ZSM-5, however, completely different changes were concluded from the V(2p) XPS spectra taken of V-ZSM-5 and Ni,V-ZSM-5. The latter case metallic vanadium was identified. Concerning the C(1s) spectra the bimetallic sample showed no signal characteristic of the VC formed. That was the main feature of V-ZSM-5.

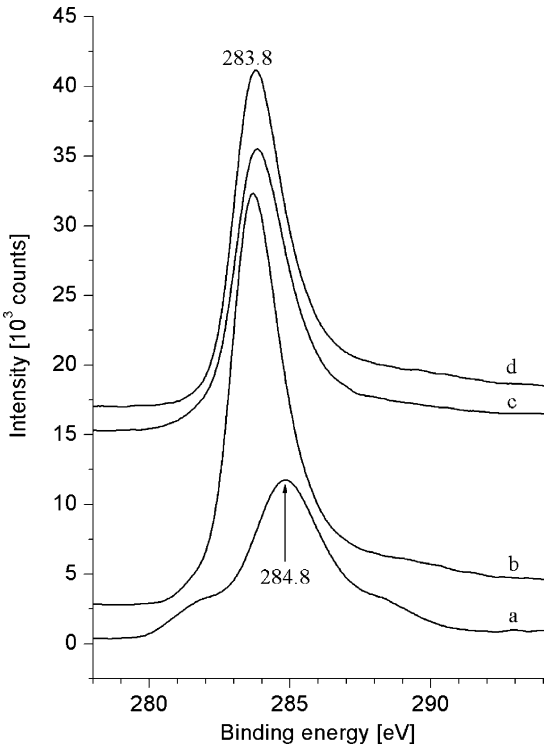

Fig. 10. XP spectra of Ni,V-ZSM-5 in C(1s) region (a) after evacuation at 300 K for 60 min, (b) after calcination at 1000 K for 20 min, (c) after 2.666 kPa C_2H_4 adsorption at 300 K for 60 min, and (d) after interaction with 2.666 kPa C_2H_4 at 1000 K for 60 min.

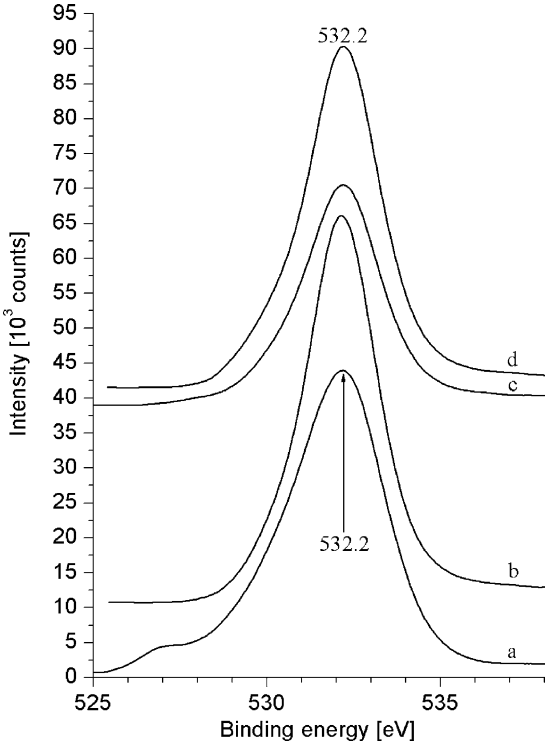

Fig. 11. XP spectra of Ni,V-ZSM-5 in O(1s) region (a) after evacuation at 300 K for 60 min, (b) after calcination at 1000 K for 20 min, (c) after 2.666 kPa C_2H_4 adsorption at 300 K for 60 min, and (d) after interaction with 2.666 kPa C_2H_4 at 1000 K for 60 min.

4. Conclusions

It is well known that different transition metal catalysts shows different properties and play different roles in carbon nanotube synthesis. Beyond the metal particles the support has also an important role. Multiwall carbon nanotubes were synthesized by CVD method on Ni-, V-, and Ni,V-ZSM-5 catalysts. Although the single metal containing catalysts resulted in nanotubes, using binary mixtures the production was much better. From the XPS results it can be concluded that the formation of metallic vanadium enhances the activity of the Ni containing catalysts.

Acknowledgements

Authors thank the financial help of the Magyary postdoctoral fellowship (Z.K.) and of the Hungarian Ministry of Education (FKFP 216/2001, OTKA T037952 and F038249).

References

[1] S. Iijima, Nature 354 (1991) 56–58.
[2] S. Iijima, T. Ichihashi, Nature (London) 363 (1993) 603.
[3] D.S. Bethune, C.H. Kiang, M.S. Devries, G. Gorman, R. Savoy, J. Vazquez, R. Beyers, Nature 363 (1993) 605–607.
[4] A. Thess, R. Lee, P. Nikolaev, P. Dai, P. Petit, J. Robert, C. Xu, Y.H. Lee, S.G. Kim, A.G. Rinzler, D.T. Colbert, G.E. Scuseria, D. Tomanek, J.E. Fisher, R.E. Smalley, Science 273 (1996) 483.
[5] T.W. Ebbesen, P.M. Ajayan, Nature 358 (1992) 220.
[6] V. Ivanov, J.B. Nagy, P. Lambin, A. Lucas, X.B. Zhang, X.F. Zhang, D. Bernaerts, G. Van Tendeloo, S. Amelinckx, J. Van Landuyt, Chem. Phys. Lett. 223 (1994) 329.
[7] K. Mukhopadhyay, A. Koshio, T. Sugai, N. Tanaka, H. Shinohara, Z. Kónya, J.B. Nagy, Chem. Phys. Lett. 303 (1999) 117.
[8] A.M. Zhang, C. Li, S.L. Bao, Q.H. Xu, Microporous Mesoporous Mater. 29 (1999) 383.
[9] I. Willems, Z. Kónya, J.-F. Colomer, G. Van Tendeloo, N. Nagaraju, A. Fonseca, J.B. Nagy, Chem. Phys. Lett. 317 (2000) 71.
[10] Z. Kónya, J. Kiss, A. Oszkó, A. Siska, I. Kiricsi, Phys. Chem. Chem. Phys. 3 (1) (2001) 155–158.
[11] Z. Kónya, I. Vesselenyi, K. Lazar, J. Kiss, I. Kiricsi, SPIE Proc. 5118 (2003) 296–304.
[12] A. Kukovecz, I. Willems, Z. Kónya, A. Siska, I. Kiricsi, Phys. Chem. Chem. Phys. 2 (2000) 3071.
[13] E.P. Barrett, L.G. Joyner, P.P. Halenda, J. Am. Chem. Soc. 73 (1951) 373.
[14] Handbook of X-Ray Photoelectron Spectroscopy, Perkin-Elmer Corporation, Physical Electronics Division, 1978, p. 80.
[15] K. Kishi, K. Fujiwara, J. Electron. spectrosc. Relat. Phenom. 85 (1997) 123.
[16] M. Demeter, M. Neumann, W. Reichelt, Surf. Sci. 454–456 (2000) 41.
[17] J.-G. Choi, Appl. Surf. Sci. 148 (1999) 64.
[18] M. Petras, B. Wichterlova, J. Phys. Chem. 96 (1992) 1805.
[19] A.V. Kucherov, A.A. Slinkin, Zeolites 7 (1987) 38.
[20] P.R.H.P. Rao, R. Kumar, A.V. Ramaswamy, P. Ratnasamy, Zeolites 13 (1993) 663.
[21] A.V. Kucherov, A.A. Slinkin, J. Mol. Catal. 90 (1994) 323.
[22] G. Went, L. Leu, R. Rosin, A. Bell, J. Catal. 134 (1992) 492.